



HAL
open science

In-situ fiber drawing induced synthesis of silver-tellurium semiconductor compounds

Clément Strutynski, Christine Labrugère, Angeline Poulon-Quintin, Marc Dussauze, Frédéric Adamietz, Thierry Cardinal, Sylvain Danto

► **To cite this version:**

Clément Strutynski, Christine Labrugère, Angeline Poulon-Quintin, Marc Dussauze, Frédéric Adamietz, et al.. In-situ fiber drawing induced synthesis of silver-tellurium semiconductor compounds. *Journal of Non-Crystalline Solids*, 2020, 543, 120159 (6 p.). 10.1016/j.jnoncrysol.2020.120159 . hal-02866105

HAL Id: hal-02866105

<https://hal.science/hal-02866105>

Submitted on 12 Jun 2020

HAL is a multi-disciplinary open access archive for the deposit and dissemination of scientific research documents, whether they are published or not. The documents may come from teaching and research institutions in France or abroad, or from public or private research centers.

L'archive ouverte pluridisciplinaire **HAL**, est destinée au dépôt et à la diffusion de documents scientifiques de niveau recherche, publiés ou non, émanant des établissements d'enseignement et de recherche français ou étrangers, des laboratoires publics ou privés.

In-situ fiber drawing induced synthesis of silver-tellurium semiconductor compounds

C. Strutynski,¹ C. Labrugère,² A. Poulon-Quintin,¹ M. Dussauze,³ F. Adamietz,³ T. Cardinal,¹ S. Danto,^{1*}

¹CNRS, Univ. Bordeaux, Bordeaux INP, ICMCB, UMR 5026, F-33600 Pessac, France

²PLACAMAT, UMS 3626, CNRS-University of Bordeaux, F-33600 Pessac, France

³Institute of Molecular Science (ISM), UMR 5255 CNRS-University of Bordeaux, 33405 Talence, France

[*sylvain.danto@u-bordeaux.fr](mailto:sylvain.danto@u-bordeaux.fr)

ABSTRACT

We examine the thermal drawing of zinc tellurite silver-containing glass. While the silver-doped glass fibers remain unchanged over thermal drawing under oxygen atmosphere, we establish that under argon silver doping leads to the growth of a thin, metallic-like precipitate at the fiber surface. Optical, chemical and structural analysis, supported by UV-vis, HR-TEM and XPS, reveals that the precipitate contains silver telluride nanoparticles in its first tens-of-nanometers. We believe the direct fiber-drawing induced synthesis of silver telluride semiconductor compounds could lead to development of new fiber-based devices, with applications spanning photonics or sensing.

Key-words Tellurite glass – Silver – Silver telluride – Fiber - XPS

1. INTRODUCTION

Optical fibers have long remained as mono-dimensional devices made of an arbitrarily long stretch of glass. Yet, alternative have emerged recently [1, 2], enabling for the fabrication of fibers made of multiple materials, with applications spanning laser surgery [3], neuroscience probing [4], acoustics [5] and so on. Meanwhile, numerous organic or inorganic materials functionalized with semiconductors [6, 7, 8] or noble metals [9] have been specifically developed to extend the range of fiber functionalities. A different approach, not extensively considered to date, consists in using the fiber drawing itself for initiating thermally-activated chemical synthesis in the confined preform space. The preform may be viewed as a micro-reactor, with the reactive agents judiciously arranged to increase the interface between adjacent domains. Initial results reveal that it enables fabricating materials that are not generally amenable to direct fiber fabrication, such as zinc selenide semiconductor [10] or silicon [11]. Other reactions can take benefit of the thermal elongated process, such as production of nanoparticles or meter-long nanowires [12, 13], or porous fibers with tunable pore size [14].

In the current work, we report on the spontaneous tellurium reduction observed at the surface vicinity of silver-containing zinc-tellurite glasses during their thermal shaping into fibers. Thanks to their extended transmission window in the infrared (up to 6 μm) and non-linear optical properties, TeO_2 -based materials have proven to form an attractive glass matrix for the development of photonic devices operating in the mid-IR [15]. Moreover, their good shaping ability and wide range of thermally stable compositions are favorable attributes for the fabrication of multi-material fibers with innovative build-in functionalities [16]. Meanwhile, silver ions doping of oxide and non-oxide glasses has appeared as an effective approach to achieve enhanced nonlinear optical properties [17], enhanced laser emissions [18] or novel photonic circuits [9].

Recently we investigated the properties of the glasses in the system $\text{TeO}_2\text{-ZnO-Na}_2\text{O-Ag}_2\text{O}$ [19]. The effect of silver oxide addition on the fiber drawing of zinc tellurite glass is examined, both in cylindrical and in ribbon fibers. Chemical composition of the Ag-rich layer was investigated through high-resolution transmission electronic microscopy (HR-TEM) and X-Ray Photoelectron Spectroscopy (XPS). It appears that upon appropriated drawing conditions silver doping leads to the spontaneous formation of a metallic-like precipitate containing silver telluride nanoparticles onto the fiber surface.

2. EXPERIMENTAL PROCEDURE

Glass synthesis and fiber fabrication Tellurite glasses were prepared by the conventional melt-quenching technique. High purity precursors (TeO_2 , ZnO , Na_2CO_3 and AgNO_3) in powder form were inserted inside a platinum crucible. The mix was then heated up to 750°C under ambient atmosphere and kept at this temperature for 30 minutes, ensuring good homogeneity of the formed liquid. Following, the melt was poured into specifically designed brass molds preheated approximately 50°C below the glass transition temperature (T_g). Glass cylindrical rods (10 mm in diameter) as well as parallelepiped preforms ($\sim 5 \text{ mm} \times 15 \text{ mm} \times 70 \text{ mm}$) were produced. Finally, the glass was annealed at $T_g - 10^\circ\text{C}$ for 12 hours and slowly ramped down ($\sim 2^\circ\text{C}\cdot\text{min}^{-1}$) to room temperature. The thermal drawing ability of the materials was assessed using a dedicated 3-meter-high optical fiber drawing tower composed of an annular electrical furnace with a sharp temperature profile, a diameter monitor, a tension dancer and a collecting drum. The preforms were slowly fed into the furnace and the temperature was gradually increased at a rate of $10^\circ\text{C}\cdot\text{min}^{-1}$ up to $\sim 350^\circ\text{C}$ to reach the softening temperature regime of the glass. The stretching of the preforms was performed either under argon or oxygen gas flow ($3 \text{ l}\cdot\text{min}^{-1}$) to avoid any external pollution of the glass surface.

Thermal properties Thermal analysis was performed by differential thermal analysis (DSC 2920 TA Instruments) on 50 mg samples. Characteristic temperatures were measured as the inflection point of the endotherm at a heating rate of $10^\circ\text{C}/\text{min}$ (precision $\pm 2^\circ\text{C}$ for T_g and T_x measurements).

Optical properties The UV-Vis (200-800 nm) transmission spectra of carefully polished bulk samples and of as-drawn ribbon fibers were recorded with a double-beam spectrophotometer (CARY 5000 Varian). The use of chosen spatial masks allows measurements on areas as low as 4 mm^2 which is adapted to smaller size sample like glass canes. Optical attenuation levels were determined using the cutback method on meters-long single index fiber samples. Light from a $\sim 20 \text{ mW}$ 1310 or 1550 nm emitting laser source was coupled into the fiber through a $20\times$ and 0.32 numerical aperture objective. The output power was then directly measured at the other end of the fiber with an InGaAs detector for different sample lengths. Reflectivity measurements were performed on a Lamda 650 spectrometer from Perkin Elmer using the Universal Reflectance Accessory (URA). The angle of incidence was 8° and the spectral range from 250 up to 900 nm.

Electrical conductivity The electrical conductivity of the Ag-Te superficial layers was verified at room temperature by using the four-point probe technique on $200\text{-}\mu\text{m}$ -thick ribbon fiber samples.

Raman spectroscopy Raman spectra were recorded with a Xplora Horiba micro-Raman spectrometer using a 532 nm excitation line with 10 mW of incident power. Raman spectra in the range of 200–2000 cm^{-1} were recorded with a resolution of 2.5 cm^{-1} .

Crystallographic analysis The crystallographic nature of the Ag-Te superficial layers of the fibers was verified by Powder X-ray diffraction (XRD) patterns which were collected on a high-resolution diffractometer (D8 Discover Bruker). Long-run scans were performed at the surface of ribbon fibers at a glazing incidence of 3° within an angular range of $2\theta = 8-80^\circ$. The Cu-K α radiation was generated at 40 kV and 40 mA ($\lambda = 0.15418 \text{ nm}$).

High-resolution transmission electron microscope Thin foils were prepared using an EM-09100 JEOL ion slicer system operating under vacuum with a 77 K local cooling. The samples were observed perpendicularly to their surface enabling iso-thickness cross-section views. TEM study was performed using a JEM - ARM 200F Cold FEG TEM/STEM operating at 200 kV. Bright field images were used to study the morphology and the localization of crystallized phases from the extreme surface to 100 μm depth. HR-TEM images were performed to control the structure of the observed crystallized phases.

X-ray Photoelectron Spectroscopy XPS surface analysis were performed using a Thermo-Fisher Scientific K-ALPHA spectrometer with a monochromatized AlK α source ($h\nu = 1486.6 \text{ eV}$) and a 200 μm X-Ray spot size. A pressure of 10^{-7} Pa was reached in the chamber when transferring the preform previously cleaned with acetone to remove carbon. The full spectra (0 - 1100 eV) were obtained with a constant pass energy of 200 eV and high resolution spectra (i.e. C1s, O1s, Te3d, Ag3d, Zn2p $_{3/2}$, Na1s) at a constant pass energy of 40 eV. Charge neutralization was applied during analysis and sputtering was achieved through low energy Ar $^+$ ions. High-resolution spectra were quantified using the AVANTAGE software provided by Thermo-Fisher Scientific (Scofield sensitivity factors applied).

3. RESULTS AND DISCUSSION

3.1 Fiber elaboration: from cylindrical to ribbon fibers

First, we assessed the ability of the selected materials to sustain the drawing process. The glass of composition 98[80TeO $_2$ –10ZnO–10Na $_2$ O] + 2%Ag $_2$ O (mol%) was selected (hereafter TZN $_{98}$ Ag $_2$). Its thermal parameters are $T_g = 286 \text{ }^\circ\text{C}$ and $T_x = 365 \text{ }^\circ\text{C}$. A mono-index cylindrical preform was manufactured and elongated through localized thermal heating in a fiber draw-tower (see *Experimental* section and Fig. 1). A typical preform along with a fiber cross-section are presented on Fig. 1a. They exhibit an orange shade originating from platinum inclusions. This coloration is

accentuated by the silver oxide, which redshifts the bandgap edge of tellurites, but also increases platinum solubility [19]. The $\text{TZN}_{98}\text{Ag}_2$ preform was then cut into two rods which were stretched into tens-of-meters-long fiber samples under oxygen (Fig. 1b) or argon (Fig. 1c) respectively with diameters $\phi \sim 150 \mu\text{m}$. No sign of heterogeneities or inclusions was visually apparent. However, drawing under argon led to the formation of a shiny sheet onto the glass preform neck-down and onto the fiber surface. No similar surface modification could be observed in the absence of silver (glass $80\text{TeO}_2\text{-}10\text{ZnO-}10\text{Na}_2\text{O}$) or when drawing the $\text{TZN}_{98}\text{Ag}_2$ glass under oxygen.

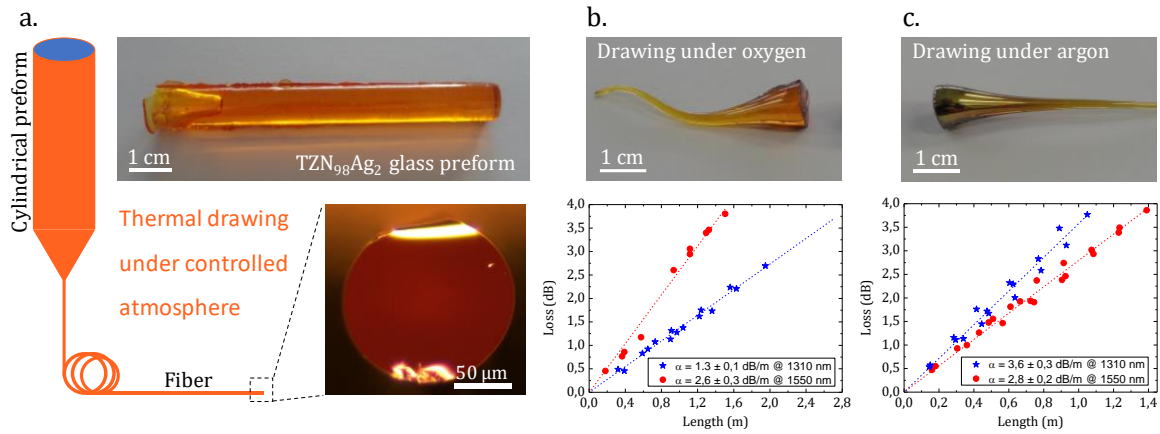


Fig. 1 (a) Fiber drawing of a $\text{TZN}_{98}\text{Ag}_2$ preform along with a fiber cross-section, (b) Glass drop obtained from drawing under oxygen and optical losses measurements at 1310 and 1550 nm, (c) Glass drop obtained from drawing under argon and optical losses measurements at 1310 and 1550 nm.

In order to confirm the optical transparency of the fibers, attenuation measurements were performed by the cutback method at 1310 and 1550 nm on initial samples of ~ 4.0 meters (Fig. 1b and Fig. 1c). Both fibers show the same attenuation level of ~ 2.7 dB/m at 1550 nm. However, at 1310 nm, the optical quality of the fiber drawn under argon deteriorates, exhibiting loss value of 3.6 dB/m, against 1.3 dB/m for the O_2 -drawn fiber. We assume that this difference originates from the layer forming at the surface of the glass elongated under argon atmosphere, which scatters and/or absorbs light at this wavelength. Although minimum loss remains relatively high for practical applications, one must note that loss was measured on bare mono-index fibers and that no purification protocol other than the use of high-purity precursors was introduced at this stage.

Then, a flat $\text{TZN}_{98}\text{Ag}_2$ preform was fabricated, carefully polished and drawn into ribbon fibers to facilitate HR-TEM and XPS surface characterizations. Drawing under argon was selected in order to promote the occurrence of a shiny, metallic-like layer at the fiber's surface. The flat preform neck-down and drop are shown in Fig. 2a. Ribbon fibers display widths ranging from $\sim 200 \mu\text{m}$ to a few millimeters (Fig. 2b, 2c). Fine control of the glass viscosity regime during the drawing allows the manufacturing of such sharp-edge thin rectangular glass structures [9].

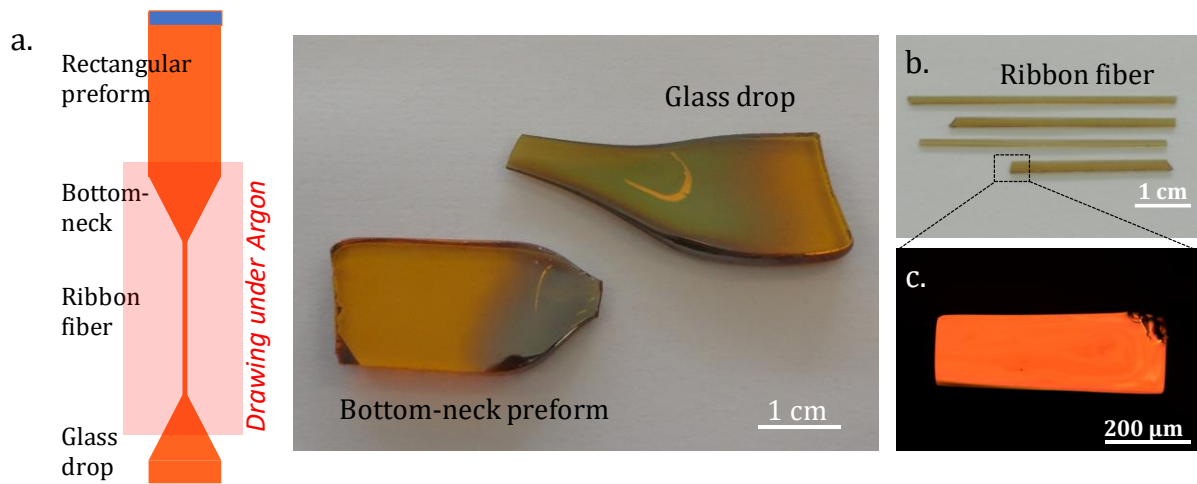


Fig. 2 (a) Flat $\text{TZN}_{98}\text{Ag}_2$ preform neck-down and drop, (b) Ribbon fibers and (c) Optical microscope view of the cross-section of a ribbon fiber

3.2 Characterization

The absorbance spectra are collected across the section of a $\text{TZN}_{98}\text{Ag}_2$ bulk material and the section of two fibers drawn under argon (fiber 1 : two faces metallized, fiber 2 : one face metallized after polishing the opposite face) (Fig. 3a). An increase of the absorbance is recorded for the 3 materials in the whole 400-800 nm range. A broad tail is noticed at the shorter wavelengths probably due to a diffusion phenomenon and a shoulder at around 540 nm, which could be related to an absorption band. In the meantime, the reflectivity of a $\text{TZN}_{98}\text{Ag}_2$ fiber metallized on both faces shows a strong reflectivity up to 35% associated with resonance at around 550 nm (Fig. 3b) which could be assigned to a material having metallic or semiconducting electrical properties. Yet, we have no evidence of the formation of a metallic layer. Plasmonic band for Ag nanoparticles in silver-containing tellurite glasses appears in region centered on 480 nm for spherical particles [20, 21]. Furthermore, XPS analysis (Figure 5) highlights a strong reduction of tellurium into Te^{2-} species.

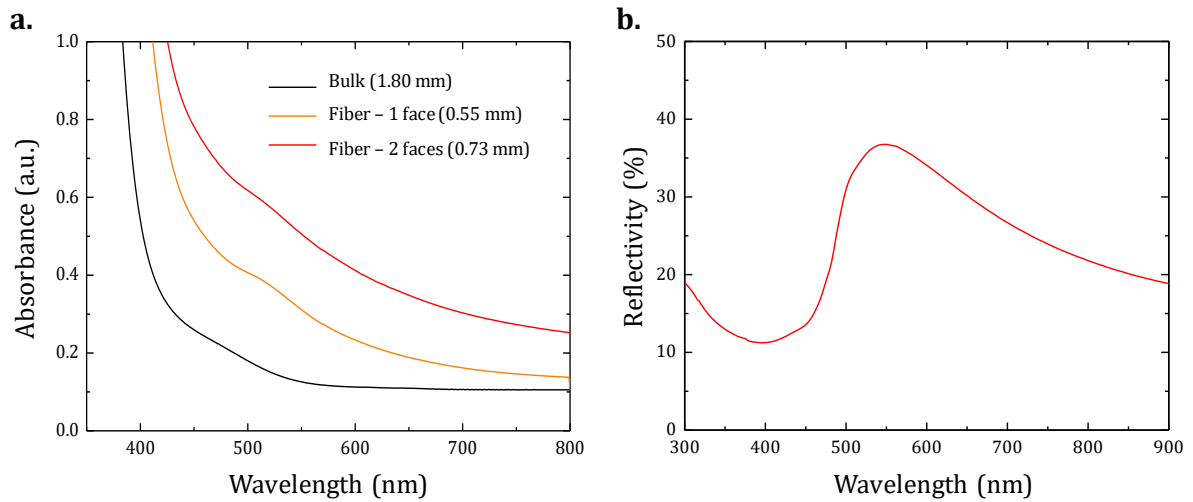


Fig. 3 (a) Absorbance spectra of TZN₉₈Ag₂ bulk (black), of a fiber metallized on two faces (red), of a fiber metallized and polished on one face (orange). (b) Reflectivity of a TZN₉₈Ag₂ fiber metallized on both faces.

A detailed investigation of the metallized surface of the TZN₉₈Ag₂ glass ribbon fiber was performed using HR-TEM (Fig. 4). HR-TEM image in bright field mode (Fig. 4a) reveals the presence of a thin amorphous layer in extreme surface (thickness: 10 ± 3 nm) covering a thicker layer (thickness: 50 ± 10 nm) of percolated nano-grains with average size spanning 5 nm to 10 nm. Fig. 4b shows image of one specific nano-grain while Fig. 4c depicts the lattice resolved HR-TEM image of the body of the precipitate. It reveals that the precipitates are actually made of three connected nanocrystals. Their respective inter-planar spacing is found to be 4.212 Å, corresponding to lattice plane [120] of Ag₂TeO₃, 2.4807 Å, corresponding to lattice plane [230] or [221] of Ag₂TeO₃, and 3.341 Å corresponding to lattice plane of [111] of Ag₂O₃. Hence, TEM analysis confirms the crystallinity of the precipitate and the larger occurrence of silver and tellurium within them.

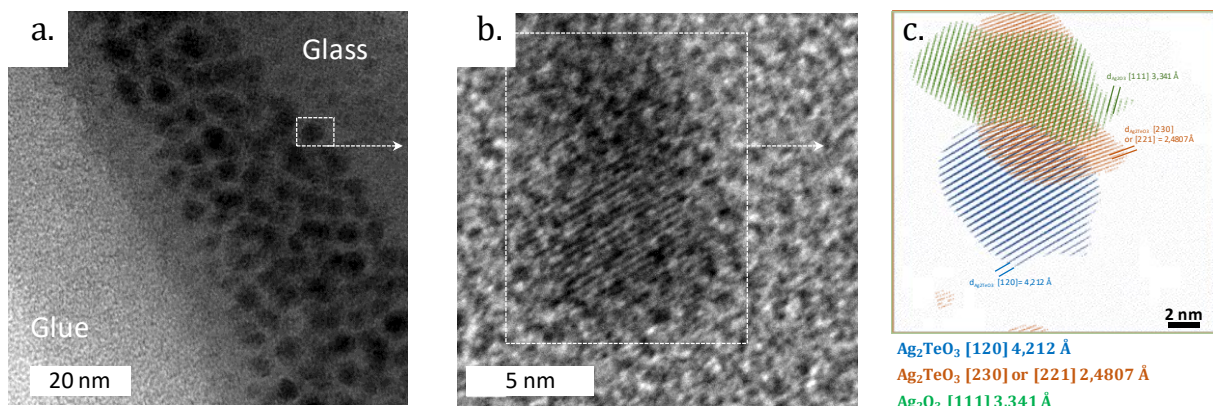


Fig. 4 (a) Bright field TEM image of the glass close to the top fiber surface (cross-sectional view), (b) HR-TEM image of one area localized inside the bilayer and used to identify the type of nano-grained compounds dispersed within the glass matrix, (c) corresponding rebuilt HR-TEM image of the body of the precipitate

In-depth XPS analysis was performed on the $\text{TZN}_{98}\text{Ag}_2$ preform neck down (Fig. 5). Nineteen measurements were performed with incremental steps up to 2200 s total sputtering. An etching rate of $0.3 \text{ nm}\cdot\text{s}^{-1}$ was applied based on a SiO_2 thin layer calibration.

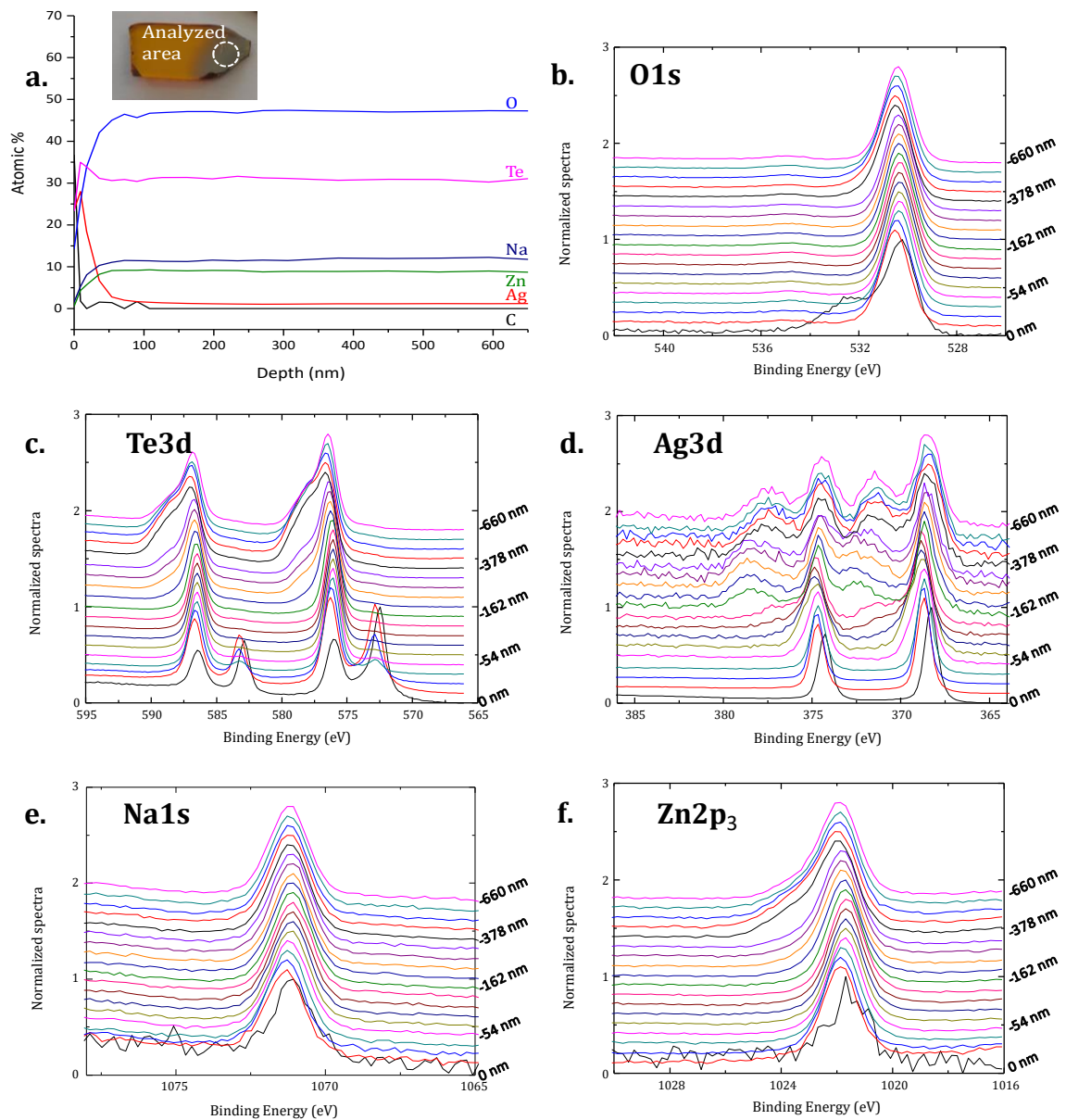


Fig. 5 : XPS sputtering on the $\text{TZN}_{98}\text{Ag}_2$ preform neck down: (a) in-depth XPS profile and high resolution spectra (b) O1s, (c) Te3d, (d) Ag3d, (e) Na1s, (f) Zn 2p_{3/2}.

A silver and tellurium rich superficial layer (thickness around 50 nm) is clearly highlighted on the depth profile (Fig. 5a) with reduced oxygen, zinc and sodium concentrations compared to the underneath glass for which a stable composition is reached (Table 1).

Table 1: XPS Atomic composition in depth for the TZN₉₈Ag₂ preform neck down

	Etching (nm)	C	O	Te	Ag	Na	Zn
Layer 1	0	36.8	14.3	23.3	23.5	1.6	0.6
	9	1.8	25.6	35.0	28.0	5.3	4.3
	18	0	33.9	33.9	18.4	8.1	5.7
	36	1.5	42.1	31.1	6.7	10.3	8.2
Layer 2	54	1.4	45.0	30.6	2.8	11.0	9.1
	90	1.6	45.6	30.4	1.6	11.5	9.1
	108	0	46.7	31.1	1.5	11.4	9.3
	162	0	47.1	31.3	1.2	11.3	9.0
Layer 3	270	0	47.3	31.2	1.0	11.6	8.8
	450	0	47.0	30.9	1.1	11.9	8.9
	666	0	47.2	31.3	1.2	11.6	8.6

In order to discuss the chemical environments, high-resolution XPS spectra related to in-depth profile are given Fig. 5b to 5f. The O1s and Na1s spectra remain unchanged (Fig. 5b and 5e). The Zn2p₃ spectra shows no major change except the appearance in depth of a shoulder at higher binding energy (Fig. 5f). Lakshminarayana *et al.* [24] observed similar spectral widening of the Zn2p₃ XPS spectra in zinc-containing borotellurite glasses that could be attributed to the formation of Zn-related complex structures inside the glass network.

The most important changes are supported by the Te3d and Ag3d spectra (Fig. 5c and 5d). For simplicity, we will further consider their 3d_{5/2} components only, since the behavior of the 3d_{3/2} component mimics that of the 3d_{5/2} one. The fiber surface exhibits two valence states for Te with two Te3d_{5/2} components at 576.0 eV and 572.5 eV (i.e. no etching). The literature quotes respectively some (TeO₃)-entities and some Te-Ag bondings (Table 2). The last species is coherent with the high rate of silver in the first tens-of-nanometers. The Ag3d_{5/2} component is located at 368.3 eV (i.e. no etching) as in Ag-Te compounds (Table 2). Due to oxygen presence in large concentration in the extreme surface (< 50 nm) we can not exclude the occurrence of oxidized Ag-Te species, in agreement with TEM (Figure 4). Deeper inside the glass (> 230 nm), a higher binding energy Te3d_{5/2} component appears at around 578.1 eV attributed to higher tellurium oxidation states such as TeO₄ groups (Table 2), which are usually part of the complex vitreous network. At

the same time, a 371.4 eV shoulder is recorded on the Ag3d_{5/2} spectra. In [30] such binding energies are attributed to Ag oxidation state and in [31] the 371.5 eV band is attributed to AgO bondings. The complex evolution of the silver valence states is assigned to its insertion inside the vitreous network.

Table 2: Binding energies review for Te3d_{5/2} and Ag3d_{5/2} XPS spectra

References	Environment	E _b (eV) Te 3d _{5/2}	E _b (eV) Ag 3d _{5/2}
Silver vanadium Tellurite glasses			
[22-24]	TeO ₄	578	
	(TeO ₃) ⁻	576	
	TeO ₃₊₁	574	
Silver-tellurium compounds			
[26]	Ag ₂ Te monoclinic	571.6	368.0
[25]	Ag ₂ Te thin films	572.4	368.2
[28]	Ag ₂ Te nanosheets	572.1 (oxide: 576.1)	368.0
[26]	Ag ₇ Te ₄ hexagonal	572.2	368.3
[27]	Ag-doped ZnTe thin films	572.6	368.2
[29]	Te-Ag (SAMs ditelluride on Ag film)	573.0	

Through various characterizations performed on the silver-doped tellurite glass fibers, we describe the material transformations occurring during the thermal drawing process as follow. Firstly, a thin silver/tellurium-rich semi-conducting or metallic discontinuous layer is formed at the extreme surface of the fiber (0 < Layer 1 < 50 nm). A gradient layer (50 nm < Layer 2 < 270 nm) is found underneath the Ag-Te rich surface This layer is rich in (TeO₃)⁻ entities which bring out the presence of a high concentration of network modifiers (here silver oxide) inside the tellurite matrix. Finally, for depth under ~270 nm (Layer 3), XPS spectra keep their overall shapes and the glass reaches its nominal structure with (TeO₃)⁻ and TeO₄ groups and some AgO entities in low concentration. The formation of a Ag-Te rich layer is allowed by the high mobility of silver ions with a small ionic radius combined with the tendency of tellurium to undergo reduction. The thermal drawing of the Ag-free 80TeO₂-10ZnO-10Na₂O glass has been extensively studied [16, 32, 33]. Yet the development of a metallic-like layer such as the one described here has never been reported. Furthermore, absorption band around 540 nm can be detected only on Ag-doped 80TeO₂-10ZnO-10Na₂O glass fiber drawn under argon. The highest density of Ag-Te nanoparticles observed at the glass surface originates first from the thermal drawing atmosphere. At drawing temperature, oxygen evaporates from the glass surface, leading to a “reductive-like” condition in the glass vicinity as oxygen is not compensate. It promotes the precipitation of

compounds in the Ag-Te system, forming nano-grains at the fiber surface. A rapid cooling occurs at the exit of the furnace, which conserve the Ag-Te nanoparticles at fiber surface. Electrical conductivity measurements performed on the layer by the 4-point probes method could not detect any signal, despite the strong metallic/semi-conducting behavior evidenced by reflectivity measurements. One believes it confirms the discontinuity of the silver-telluride layer as observed in HR-TEM images. Another explanation relies in the formation of Ag-Te precipitate mixed with oxidized Ag-Te species, in agreement with the XPS chemical concentration (Table1). Beside electrical measurements, Raman spectroscopy and XRD analysis were performed at the fiber surface. Yet, due to the thickness of the analyzed layer below 100 nm, one could not evidence any structural modification of the superficial glass layer.

Here we utilize the fiber drawing itself for initiating the thermally-activated chemical synthesis of compounds in the binary silver-tellurium system. Some silver-telluride compounds own many interesting optical and electronic properties such as large magnetoresistance and good thermoelectric properties [34]. Yet, to date, due to its crystallinity and high melting temperature ($T_m = 955\text{ °C}$), Ag_2Te was not amenable to direct fiber fabrication, precluding its insertion into fibers. The method proposed here represents an alternative route for introducing semiconducting compounds within fiber.

4. CONCLUSION

We have demonstrated the *in-situ* synthesis of semi-conducting thin layers in the system Te-Ag onto fiber activated by direct thermal drawing of a preform. The methods described herein set the stage for extending the range of semiconductor materials within fiber, representing a milestone in fiber device processing. The ability to control the synthesis of silver telluride semiconductor compounds during the fiber draw process should lead to substantial advances in the implementation of new functionalities within fibers. It could be applicable to infrared sensors, nonlinear optical devices or biological sensors for instance.

Acknowledgments

Funding for this work has been provided from the French Government, managed by the French National Research Agency (ANR Grant 62243), by the IdEx program at the University of Bordeaux, the Cluster of excellence LAPHIA and the Région Nouvelle-Aquitaine.

REFERENCES

1. G. Tao *et al.* "Multimaterial Fibers" *Internat. Jr. App. Glass Science* 3 (2012) 349
2. M. A. Schmidt *et al.* "Hybrid Optical Fibers – An Innovative Platform for In-Fiber Photonic Devices" *Adv. Optical Mater.* 4 (2016) 13
3. B. Temelkuran *et al.* "Wavelength-scalable hollow optical fibres with large photonic bandgaps for CO₂ laser transmission" *Nature* 420 (2002) 650
4. A. Canales *et al.* "Multifunctional fibers for simultaneous optical, electrical and chemical interrogation of neural circuits *in vivo*" *Nature Biotechnology* 33 (2015) 277
5. S. Egusa *et al.* "Multimaterial piezoelectric fibres" *Nature Mat.* 9 (2010) 643
6. C. Sifuentes *et al.* "Application of CdSe-nanocrystallite-doped glass for temperature measurements in fiber sensors" *Opt. Eng.* 39 (2000) 2182
7. J. Ballato *et al.* "Advancements in semiconductor core optical fiber" *Optical Fiber Techno.* 16 (2010) 399
8. R. He *et al.* "Silicon p-i-n Junction Fibers" *Adv. Mater.* 25 (2013) 1461
9. S. Danto *et al.* "Photo-writable silver-containing phosphate glass ribbon fibers" *Adv. Opt. Mat.* 4 (2016) 162
10. N. D. Orf *et al.* "Composite Diode Fibres fabricated via in-situ Compound Synthesis" *Proc. of Nat. Ac. of Sc.* 108 (2011) 4743
11. C. Hou *et al.* "Crystalline silicon core fibres from aluminium core preforms" *Nature Communications* 6 (2015) 6248
12. D. Deng *et al.* "Processing and Properties of Centimeter-long, In-fiber Crystalline-Se Filaments" *Appl. Phys. Lett.* 96 (2010) 023102
13. J. Kaufman *et al.* "Thermal Drawing of High-Density Macroscopic Arrays of Well-Ordered Sub-5-nm-Diameter Nanowires" *Nano Lett.* 11 (2011) 4768
14. B. Grena *et al.* "Thermally-drawn fibers with spatially-selective porous domains" *Nature Communications* 8 (2017) 364
15. R. H. El-Mallawany "Tellurite glasses Hand book – Physical properties and data" CRC press LLC (2002)
16. C. Strutynski *et al.* "Tellurite-based core-clad dual-electrodes composite fibers" *Opt. Mat. Express* 7 (2017) 1503
17. D. Linda *et al.* "Optical properties of tellurite glasses elaborated within the TeO₂-Tl₂O-Ag₂O and TeO₂-ZnO-Ag₂O ternary systems" *J. Alloys and Compounds* 561 (2013) 151
18. L. P. R. Kassab *et al.* "ZnO-TeO₂-Yb/Tm glasses with silver nanoparticles as laser operated quantum electronic devices" *Opt. Laser Technol.* 42 (2010) 1340
19. D. Boiruchon *et al.* "Investigation of the Na₂O/Ag₂O ratio on the synthesis conditions and properties of the 80TeO₂-10ZnO-[(10-x)Na₂O-xAg₂O] glasses" *J. Non-Crystal. Solids* 525 (2019) 119691
20. J. M. Giehl *et al.* "Thermal precipitation of silver nanoparticles and thermoluminescence in tellurite glasses" *Opt. Mater.* 33 (2011) 1884

21. S. Ukon *et al.* "Surface modification of tellurite glass by thermal poling accompanied with ion implantation in a solid-state phase" *Phys. Chem. Glasses: Eur. J. Glass Sci. Technol. B*, 49 (2008) 285
22. H. M. M. Moawad *et al.* "Electrical Conductivity of Silver Vanadium Tellurite Glasses" *J. Am. Ceram. Soc.* 85 (2002) 2655
23. A. Mekki *et al.* "XPS and magnetic studies of vanadium tellurite glasses" *J. Electron. Spectroscop.* 175 (2009) 21
24. G. Lakshminarayana *et al.* "X-ray photoelectron spectroscopy (XPS) and radiation shielding parameters investigations for zinc molybdenum borotellurite glasses containing different network modifiers" *J. Mater. Sci.* 52 (2017) 7394
25. E.K. Kim *et al.* "A facile room temperature chemical transformation approach for binder-free thin film formation of Ag₂Te and lithiation/delithiation chemistry of the film" *Dalton Trans.* 45 (2016) 17312
26. R. Chen *et al.* "Electrodeposition of silver telluride thin films from non-aqueous baths" *Electrochim. Acta* 49 (2004) 2243
27. T. Potlog *et al.* "Temperature-dependent growth and XPS of Ag-doped ZnTe thin films deposited by close space sublimation method" *Appl. Surface Science* 352 (2015) 33
28. S. Chen *et al.* "TOP as ligand and solvent to synthesize silver telluride nanosheets" *Mater. Res. Bulletin* 71 (2015) 30
29. T. Weidner *et al.* "Self-Assembled Monolayers of Aromatic Tellurides on (111)-Oriented Gold and Silver Substrates" *J. Phys. Chem. C* 111 (2007) 11627
30. X. Yuqing *et al.* "Atomic force microscopy and X-ray photoelectron spectroscopy study on nanostructured silver thin films irradiated by atomic oxygen" *Mater. Sci. Eng. B* 49 (2001) 68
31. A. M. Ferraria *et al.* "X-ray photoelectron spectroscopy: silver salts revisited" *Vacuum* 86 (2012) 1988
32. A. Belwalkara *et al.* "Extruded tellurite glass optical fiber preforms" *J. Materials Process. Tech.* 210 (2010) 2016
33. S. Manning *et al.* "Ternary tellurite glasses for the fabrication of nonlinear optical fibres" *Optical Mat. Express* 2 (2012) 140
34. C.S. Suchand Sandeep *et al.* "Optical limiting properties of Te and Ag₂Te nanowires" *Chemical Physics Letters* 485 (2010) 326